Low-Cost Electrical Beam-Scanning Leaky-Wave Antenna Based on Bent Corrugated Substrate Integrated Waveguide

Tian Lou, Xue-Xia Yang, *Senior Member, IEEE*, Houtong Qiu, Qi Luo, and Steven Gao, *Senior Member, IEEE*

***Abstract*—This letter presents a novel low-cost leaky-wave antenna (LWA) with the fixed-frequency beam-scanning capability. An improved half-mode corrugated substrate integrated waveguide structure is proposed as the guiding wave structure to reduce the transverse size of the antenna. A novel electronic phase-shifting structure, composed of fan-shaped open stubs with different sizes and PIN diodes, is proposed for beam scanning. This LWA uses interdigital slots as radiating elements, and the phase-shifting structure is placed between the adjacent radiating elements. By changing the switching states of these PIN diodes, the phase difference between the adjacent radiating elements can be controlled. To verify the concept, one prototype of the 2 × 6 array antenna at *C*-band is designed, simulated, fabricated, and measured. The antenna demonstrates a beam-scanning range of 25° (34°–59°) at fixed frequency, a peak gain of 12.4 dBi with the gain variation less than 2.3 dB. The antenna has low cost and can be easily fabricated using standard printed circuit board process.**

***Index Terms*—Beam-scanning antenna, leaky-wave antenna (LWA), PIN diode, substrate integrated waveguide.**

I. Introduction

With the advantages of saving power, high security, and decreasing interferences, beam-scanning antennas are required in many civilian and military applications [1], [2]. Since the first known microstrip planar leaky-wave antenna (LWA) invented in the late 1970s, the planar LWA has attracted increasing attention because of its simple feeding network, low profile, and frequency-scanning capability. Recently, based on LWA, different types of frequency-scanning antenna were proposed, such as microstrip LWAs [3], [4], substrate integrated waveguide (SIW) LWAs [5], [6], and parallel-plate waveguide LWA [7]. However, the frequency-scanning antennas need a wide operation band, which is not suitable for most wireless communication systems.

By loading binary switches and metal shorted patches on the half-width microstrip line, a LWA with beam-scanning operating at a fixed frequency in *C*-band was demonstrated in [8]. A beam-scanning LWA operating at 2.4 GHz was proposed in [9] by using metamaterial-based phase shifters. Another solution to achieve beam scanning at a fixed frequency is loading varactors between the radiation elements [10]. The SIW technology brings the benefits of changing the traditional rectangular waveguide to the planar microwave integrated circuit technology [11]. Due to its well-known features of light weight, low profile, low cost, and ease of fabrication, the SIW is suitable for designing the LWA [12]–[14]. However, the top and bottom conductors of the SIW are not dc isolated because they are connected by the metallic vias. Thus, the SIW is not convenient for dc bias and integration of active devices. Chen and Eccleston [15] proposed the corrugated SIW (CSIW), which uses open-circuit quarter-wavelength microstrip stubs in place of metallic vias to artificially create the electric sidewalls and maintain the dc isolation between the top and bottom conductors. This structure can support the same TE_{10} mode as the SIW and is easy to integrate with active components [16]. However, CSIW has a wide transverse dimension, which is not suitable for the array design. In order to reduce the transverse size of the CSIW, an improved CSIW structure, denoted the bent CSIW (BCSIW), is proposed in this letter. By using a bent open-circuit quarter-wavelength microstrip stub, the size of the CSIW is reduced by about 17%.

In this letter, based on the proposed BCSIW structure, a LWA with fixed-frequency beam-scanning capability is designed. This LWA uses interdigital slots as the radiating elements, and scans its main beam at a fixed frequency by placing phase-shifting structures between adjacent radiating elements. In order to combine the phase-shifting structure with the LWA, half-mode BCSIW (HM-BCSIW) is used in this design. A novel electronic phase-shifting structure, which mainly consists of four fan-shaped open microstrip stubs of different sizes and six PIN diodes, is connected to the free edge of the HM-BCSIW. The beam scanning is achieved by changing the dc bias voltages of the six PIN diodes on each phase-shifting structure. A prototype antenna was simulated, fabricated, and measured to validate the proposed design. Because the top and bottom con-

Manuscript received November 19, 2018; revised December 17, 2018; accepted December 27, 2018. Date of publication January 4, 2019; date of current version February 1, 2019. This work was supported by the National Natural Science Foundation of China under Grant 61771300. *(Corresponding author: Tian Lou.)*

T. Lou and H. Qiu are with the School of Communication and Information Engineering, Shanghai University, Shanghai 200072, China (e-mail: loutian@shu.edu.cn; 810970463@qq.com).

X.-X. Yang is with the Key Laboratory of Specialty Fiber Optics and Optical Access Networks, Shanghai Institute for Advanced Communication and Data Science, Shanghai University, Shanghai 200444, China (e-mail: yang.xx@shu.edu.cn).

Q. Luo and S. Gao are with the School of Engineering and Digital Arts, University of Kent, Canterbury CT2 7NZ, U.K. (e-mail: Q.Luo@kent.ac.uk; S.Gao@kent.ac.uk).

Digital Object Identifier 10.1109/LAWP.2019.2890995

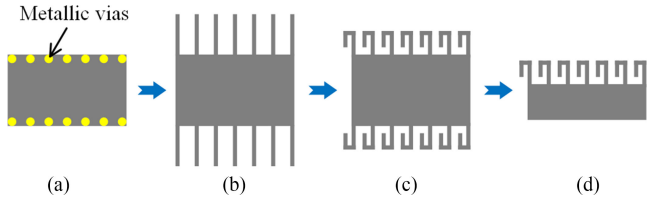

Fig. 1. Evolution of the HM-BCSIW. (a) SIW, (b) CSIW, (c) BCSIW, (d) HM-BCSIW.

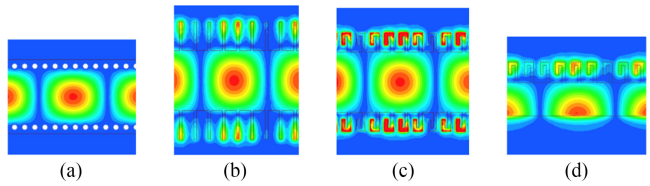

Fig. 2. Electrical field distributions of (a) SIW, (b) CSIW, (c) BCSIW, and (d) HM-BCSIW at 5.8 GHz.

ductors of this antenna are dc isolated, it can be easily combined with other active components and devices.

II. Antenna Design and Analysis

A. HM-BCSIW Guiding Wave Structure Evolution

Fig. 1 shows the evolution of the proposed HM-BCSIW. The CSIW uses open-circuit quarter-wavelength microstrip stubs [see Fig. 1(b)] in place of the metallic vias in the conventional SIW [see Fig. 1(a)] to artificially create the electric sidewalls and maintain the dc isolation between the top and bottom conductors [15]. By using the bent open-circuit quarter-wavelength microstrip stubs [see Fig. 1(c)], the transverse size of the CSIW is reduced, which is denoted as BCSIW. In order to further reduce the size of the CSIW and connect to the phase-shifting structures in the subsequent antenna design, the HM-BCSIW structure [see Fig. 1(d)] is suggested.

Fig. 2 shows the electrical field distributions of the four SIW structures at 5.8 GHz. Those of the CSIW and BCSIW are similar to that of the traditional SIW, which show they operate on the same mode of TE_{10}. Correspondingly, the operation mode for HM-BCSIW is the $TE_{0.5,1}$ mode. Both the bent open-circuit quarter-wavelength microstrip stub and the straight one form the artificial electric sidewalls.

B. HM-BCSIW Beam-Scanning LWA Design

Fig. 3 shows the configuration of the proposed electrical beam-scanning LWA. The substrate used for this design is F4B with the relative permittivity of 2.2 and loss tangent of 0.001. The substrate thickness is 1.5 mm. The antenna is composed of the HM-BCSIW LWA, the electronic phase-shifting structure, and the microstrip to HM-BCSIW transition structure.

The LWA uses HM-BCSIW as the guiding wave structure. Referring to the SIW-based LWA design in [12], by etching interdigital slots on the top conductor of the HM-BCSIW as the radiating elements, an HM-BCSIW LWA is developed. Two HM-BCSIW LWAs are placed symmetrically for increasing the antenna gain. An electronic phase-shifting structure

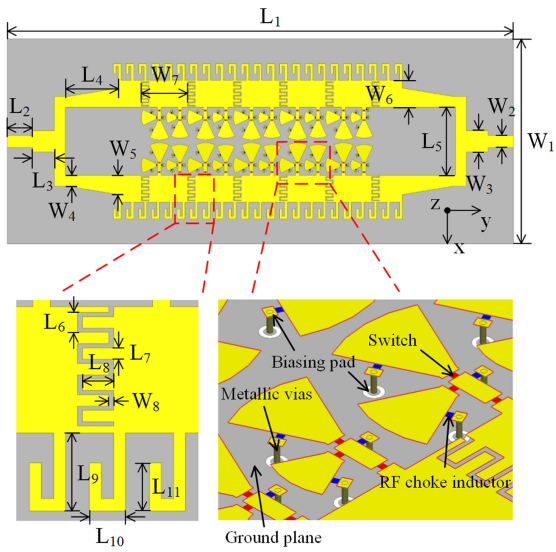

Fig. 3. Configuration of the proposed electrical beam-scanning LWA.

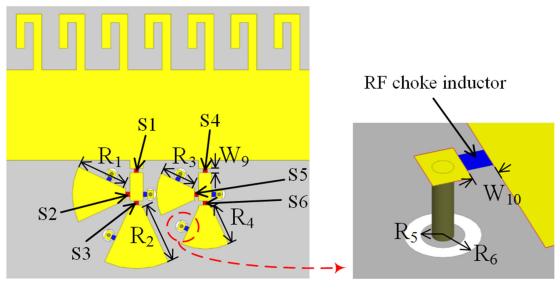

Fig. 4. Configuration of the electronic phase-shifting structure.

is placed between adjacent radiating elements for the fixed-frequency beam-scanning capability of the LWA. By electrically changing the phase difference between adjacent radiating elements, the beam scanning is achieved. There are 2×6 radiating elements and 2×5 phase-shifting structures in the prototyped antenna.

The microstrip-to-HM-BCSIW transition structure, which includes a 50 Ω microstrip line, a microstrip power divider, and a tapered microstrip line, is used as feed structure of the LWA. The tapered microstrip line is used to excite the TE_{10} mode of the HM-BCSIW. By optimizing the widths W_4, W_5 and the length L_4 of the tapered microstrip line, the structure can achieve a good impedance matching. The antenna is fed from one end, and the other end is terminated with a 50 Ω coaxial load to suppress the reflected waves.

The detailed dimensions of the proposed electronic phase-shifting structure are shown in Fig. 4. The phase-shifting structure is composed of two-phase shifting units, while each phase shifting unit consists of two fan-shaped open stubs with different sizes. In order to make the structure compact, the two fan-shaped open stubs are positioned perpendicularly to each other and are connected to a rectangular patch of 1.5 mm × 3.25 mm in size by binary switches. The patch is connected to the free edge of the HM-BCSIW by a binary switch and a microstrip line of 1.5 mm × 1 mm in size. The dimensions of the four fan-shaped open stubs used in the electronic phase-shifting structure are R_1, R_2,

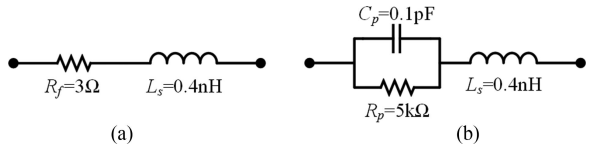

Fig. 5. Simulation models of PIN diode in (a) "ON" and (b) "OFF" states.

R_3, and R_4, respectively, and the binary switches are numbered as $S1$–$S6$, whose positions are shown in Fig. 4. The PIN diode is used as the binary switch in this design. The switching state of the PIN diode is controlled by the dc bias voltages. A dc biasing circuit is designed to independently control the switching state of each PIN diode. The dc biasing circuit consists of the RF choke inductors, the top biasing pads, the bottom biasing pads, and the metallic vias. The bottom biasing pads are separated from the ground plane by etching annular slots. The dc bias voltages supply is on the bottom biasing pads to minimize the effect of dc circuits on the antenna RF performance. The widths of the slits for placing the PIN diode and the RF choke inductor are W_9 and W_{10}, respectively.

The operation principle of the electronic phase-shifting structure is as follows. The phase-shifting structure is connected to the HM-BCSIW. By controlling the states of the binary switches $S1$–$S6$, the numbers and sizes of the fan-shaped open stubs loaded on the HM-BCSIW are different. Because the parallel reactances introduced by the different number and size of the stubs are different, the phase shift could be achieved. For example, when switches $S1$ and $S2$ are set to "ON" state and switches $S3$–$S6$ are set to "OFF" state, the loading on the HM-BCSIW is the stub with the size of R_1. When switches $S2$ and $S5$ are set to "OFF" state and the other switches are set to "ON" state, the loading on the HM-BCSIW is the two stubs with the size of R_2 and R_4. The "ON" and "OFF" states of each switch are denoted as "1" and "0," respectively. Thus, the operation states of this electronic phase-shifting structure can be described by using a 6 bit binary code. There are two steps of designing the phase-shifting structure. First, determine the phase shifts for different beam-scanning angles. Second, confirm the switch states and optimize the size of four fan-shaped open stubs of R_1, R_2, R_3, and R_4.

C. Simulation Analysis

The PIN diode used in the simulation and measurement are BAR50-02L from Infineon Company. The equivalent circuit model used in the simulation is shown in Fig. 5. To illustrate the beam-scanning effect of the antenna with different values and numbers of fan-shaped open stubs, Fig. 6 shows the radiation patterns with different values of R_4 for the switch states of "000101" and "101101." When the size of the fan-shaped open stub R_4 varies from 3.6 to 7 mm, the scan-angle ranges corresponding to the switch states "000101" and "101101" are 45°–52° and 39°–46°, respectively.

The simulated reflection coefficients for different switching states are plotted in Fig. 7. The simulated bandwidth for these switching states of the reflection coefficient less than −10 dB is 5.72–6.16 GHz. Fig. 8 shows the radiation patterns of these switching states at the operation frequency of 5.8 GHz. As can

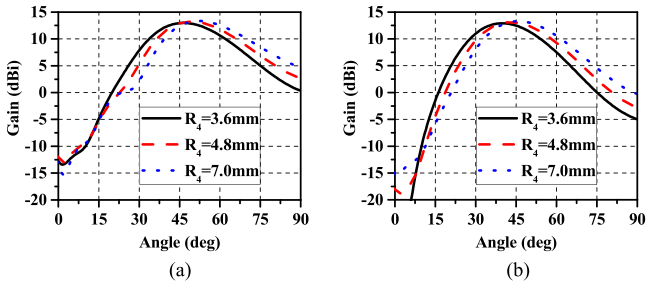

Fig. 6. Radiation pattern with different values of R_4. (a) "000101" state. (b) "101101" state. (The sizes of R_1, R_2, and R_3 are unchanged with the values of 5.4, 7.1, and 3.6 mm, respectively.)

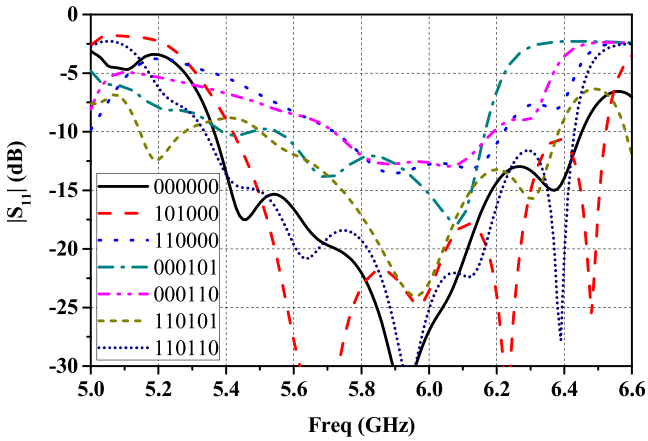

Fig. 7. Simulated reflection coefficients of the proposed antenna for different switching states.

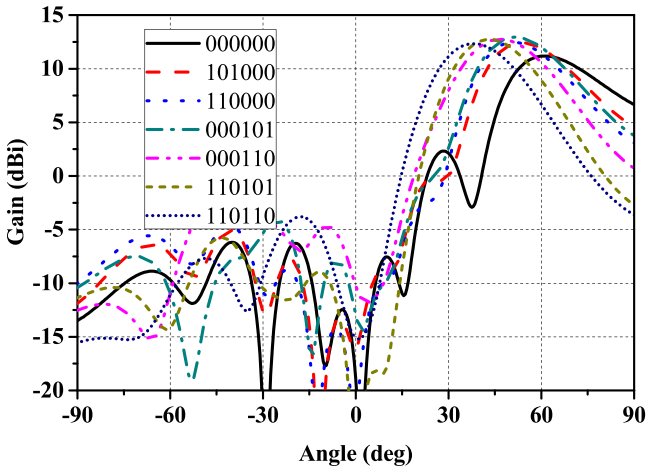

Fig. 8. Simulated radiation patterns of the proposed antenna for different switching states at 5.8 GHz.

be seen, the main beam directions for some switching states are almost the same. For example, the main beam direction for switching states of "110000" and "000101" are 51° and 51.5°, respectively, which are very close to each other. Therefore, in practice, only parts of the switching states are useful. Considering the reflection coefficient of different switching states, five states corresponding to different scanning angles are selected as the preset scanning states of the antenna, which are "000000," "101000," "000101," "110101," and "110110." The maximum

TABLE I
DIMENSIONS OF THE ANTENNA (UNIT: mm)

L_1	L_2	L_3	L_4	L_5	L_6	L_7	L_8	L_9
198	10	8.5	20	26.6	1.65	0.95	2.6	6.5
L_{10}	L_{11}	W_1	W_2	W_3	W_4	W_5	W_6	W_7
3	4	80	4.6	8.5	4.2	7.5	10.5	18
W_8	W_9	W_{10}	R_1	R_2	R_3	R_4	R_5	R_6
0.4	0.5	0.5	5.4	7.1	3.6	6.4	0.4	0.7

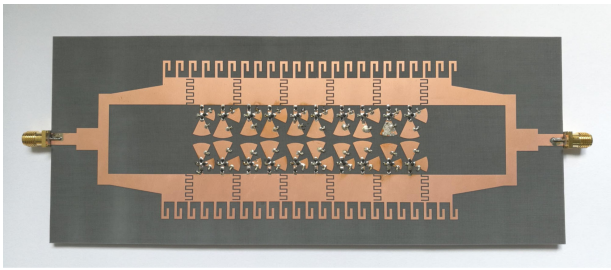

Fig. 9. Photograph of the fabricated antenna.

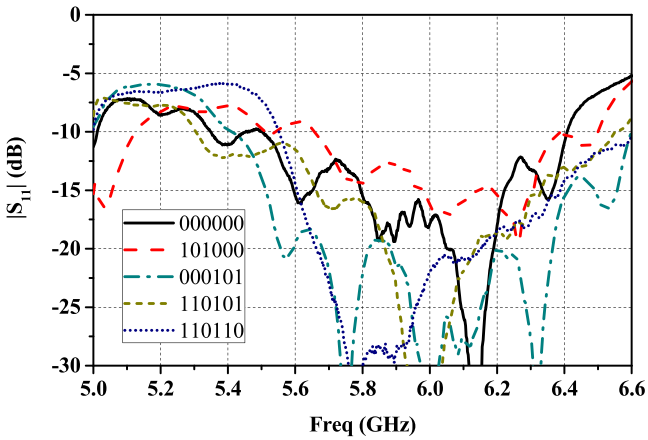

Fig. 10. Measured reflection coefficients of the proposed LWA for the five preset scanning states.

simulated gain of these five states is 12.9 dBi. Within the scan-angle ranges from 37° to 61°, the scanning gain variation is less than 1.8 dB. The simulated radiation efficiencies of all these preset switching states are above 85% at 5.8 GHz. In addition, the main beam direction has a slight shift toward higher angle with the frequency increases, which results from the series-fed traveling-wave structure of the antenna array.

III. MEASUREMENT AND DISCUSSION

To evaluate the performance of the proposed LWA, a prototype was fabricated and measured. Table I lists the main dimensions of the antenna. Fig. 9 shows the photograph of the fabricated antenna.

The measured reflection coefficients for the five preset scanning states are plotted in Fig. 10. The measured −10 dB reflection coefficient bandwidth for these switching states is 5.66–6.41 GHz. The difference between the simulation and measurement is mainly caused by the parameter errors between the real PIN diode and the equivalent circuit model used in the

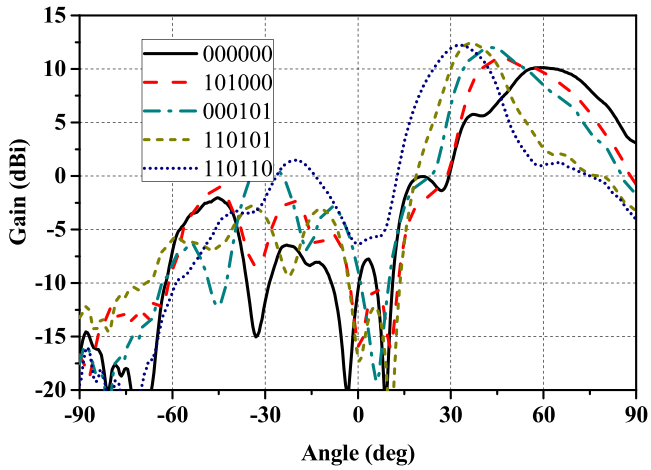

Fig. 11. Measured radiation patterns of the proposed LWA for the five preset scanning states at 5.8 GHz.

simulation. The manufacturing and measurement error is another reason for this difference.

The measured radiation patterns of these preset scanning states are shown in Fig. 11. It is seen that the measured scan angles of these states agree to the simulated ones. At the operation frequency of 5.8 GHz, the antenna achieves a maximum gain of 12.4 dBi. The measured gain is slightly lower than the simulated one, which is mainly caused by the parasitic parameters of the PIN diode and the manufacturing errors. The switching states corresponding to the maximum and minimum scan angles of the antenna are "000000" and "110110," respectively. The measured scan-angle range is 34°–59° with the scanning gain variation less than 2.3 dB.

The scan-angle range of this LWA is limited by the phase-shifting range of the electronic phase-shifting structure. In future research, the scan-angle range can be increased by using other lump components, such as varactors and inductor tunable elements.

IV. CONCLUSION

Based on the HM-BCSIW structure, a beam-scanning LWA operating at *C*-band is proposed in this letter. The novel contributions from this letter lie in two points. First, an improved CSIW structure is proposed. By using a bent open-circuit quarter-wavelength microstrip stub instead of the straight stub, the improved structure can maintain the dc isolation between the top and bottom conductors of the SIW, while the size is reduced by about 17% compared to the original CSIW design. Second, a fixed-frequency beam-scanning method for LWA is proposed. A novel electronic phase-shifting structure, which consists of fan-shaped open stubs and PIN diodes, are placed between the radiating elements of the LWA for the capability of beam scanning. A prototype antenna was fabricated and measured. At the operation frequency of 5.8 GHz, the antenna achieves a measured scan-angle range of 25° with the maximum gain of 12.4 dBi and the gain variation less than 2.3 dB. Due to the characteristics of compact structure and low profile, the proposed antenna is potentially useful for modern wireless communication systems.

REFERENCES

[1] Y. Rahmat-Samii and A. C. Densmore, "Technology trends and challenges of antennas for satellite communication systems," *IEEE Trans. Antennas Propag.*, vol. 63, no. 4, pp. 1191–1204, Apr. 2015.

[2] S. Gao, Y. Rahmat-Samii, R. E. Hodges, and X. Yang, "Advanced antennas for small satellites," *Proc. IEEE*, vol. 106, no. 3, pp. 391–403, Mar. 2018.

[3] Y. Li, Q. Xue, H. Tan, and Y. Long, "The half-width microstrip leaky wave antenna with the periodic short circuits," *IEEE Trans. Antennas Propag.*, vol. 59, no. 9, pp. 3421–3423, Sep. 2011.

[4] S. A. K. Tanoli, M. I. Khan, Q. Fraz, X. Yang, and S. A. Shah, "A compact beam-scanning leaky-wave antenna with improved performance," *IEEE Antennas Wireless Propag. Lett.*, vol. 17, no. 5, pp. 825–828, May 2018.

[5] A. Pourghorban Saghati, M. M. Mirsalehi, and M. H. Neshati, "A HM-SIW circularly polarized leaky-wave antenna with backward, broadside, and forward radiation," *IEEE Antennas Wireless Propag. Lett.*, vol. 13, pp. 451–454, 2014.

[6] Y. Lyu *et al.*, "Leaky-wave antennas based on noncutoff substrate integrated waveguide supporting beam scanning from backward to forward," *IEEE Trans. Antennas Propag.*, vol. 64, no. 6, pp. 2155–2164, Jun. 2016.

[7] Y. You, Y. L. Lu, G. M. Xu, Q. C. You, and J. F. Huang, "Frequency-scanned antenna array based on continuous transverse stub," in *Proc. Prog. Electromagn. Res. Symp.*, 2017, pp. 1470–1473.

[8] D. K. Karmokar, K. P. Esselle, and S. G. Hay, "Fixed-frequency beam steering of microstrip leaky-wave antennas using binary switches," *IEEE Trans. Antennas Propag.*, vol. 64, no. 6, pp. 2146–2154, Jun. 2016.

[9] Y. Li, M. F. Iskander, Z. Zhang, and Z. Feng, "A new low cost leaky wave coplanar waveguide continuous transverse stub antenna array using metamaterial-based phase shifters for beam steering," *IEEE Trans. Antennas Propag.*, vol. 61, no. 7, pp. 3511–3518, Jul. 2013.

[10] E. Abdo-Sánchez, D. Palacios-Campos, C. Frías-Heras, F. Y. Ng-Molina, T. M. Martín-Guerrero, and C. Camacho-Peñalosa, "Electronically steerable and fixed-beam frequency-tunable planar traveling-wave antenna," *IEEE Trans. Antennas Propag.*, vol. 64, no. 4, pp. 1298–1306, Apr. 2016.

[11] M. Bozzi, A. Georgiadis, and K. Wu, "Review of substrate-integrated waveguide circuits and antennas," *Microw., Antennas Propag.*, vol. 5, no. 8, pp. 909–920, Jun. 2011.

[12] Y. Dong and T. Itoh, "Composite right/left-handed substrate integrated waveguide and half mode substrate integrated waveguide leaky-wave structures," *IEEE Trans. Antennas Propag.*, vol. 59, no. 3, pp. 767–775, Mar. 2011.

[13] W. Cao, Z. N. Chen, W. Hong, B. Zhang, and A. Liu, "A beam scanning leaky-wave slot antenna with enhanced scanning angle range and flat gain characteristic using composite phase-shifting transmission line," *IEEE Trans. Antennas Propag.*, vol. 62, no. 11, pp. 5871–5875, Nov. 2014.

[14] S. S. Haghighi, A. Heidari, and M. Movahhedi, "A three-band substrate integrated waveguide leaky-wave antenna based on composite right/left-handed structure," *IEEE Trans. Antennas Propag.*, vol. 63, no. 10, pp. 4578–4582, Oct. 2015.

[15] D. G. Chen and K. W. Eccleston, "Substrate integrated waveguide with corrugated wall," in *Proc. Asia-Pacific Microw. Conf.*, 2008, pp. 1–4.

[16] K. W. Eccleston, "Corrugated substrate integrated waveguide distributed amplifier," in *Proc. Asia Pacific Microw. Conf.*, 2012, pp. 379–381.